FATIGUE DAMAGE EVOLUTION IN $[0_F/90_{U,3}/0_F]$ COMPOSITE TUBES UNDER MULTIAXIAL LOADING

P.A. Carraro, M. Quaresimin*
Department of Management and Engineering, University of Padova, Stradella S. Nicola 3, Vicenza, Italy
* marino.quaresimin@unipd.it

Keywords: *multiaxial fatigue, composites, mixed mode, damage mechanisms*

Abstract
Results of an extensive experimental investigation on multiaxial fatigue behavior of $[0_F/90_{U,3}/0_F]$ glass/epoxy tubes are presented and discussed. Specimens are subjected to combined tension-torsion loadings, resulting in the stress components σ_2 and τ_{12} in the 90° layers of the tubes. The effect of shear stress on damage mechanics has been investigated and a strong influence on both damage onset and propagation has been observed. SEM investigation of fracture surfaces shows the dependence of damage modes, at the microscopic scale, on the multiaxiality condition. Comparison with previous results on tubes with different lay-up ($[90_{U,4}]$, $[0_F/90_{U,3}]$) shows the strong influence of the constraining 0° fabric layers on the damage onset and propagation.

1 Introduction

Multiaxial fatigue behavior of composite materials has received little attention so far by the scientific community. Just few life prediction criteria can be found in the literature; some of them were analyzed and compared to experimental data [1], obtaining not always satisfactory results. The analyses conducted in [1] showed the inaccuracy of empirical criteria and the deep lack of information about the damage modes and their dependence on the multiaxiality condition. In order to define a reliable prediction model it is important to understand and describe quantitatively the damage mechanisms and their nucleation and propagation till the final failure. Only few papers in the literature report quantitative analyses on the damage growth [2,3], while qualitative analyses can be found in [4-8]. The aim of this work is to investigate the damage mechanisms of glass/epoxy composite tubes subjected to a cyclic loading condition resulting in a non-fiber-dominated behavior. For this purpose glass epoxy tubes are tested under combined tension/torsion cyclic loadings, and the experimental results are compared to those presented in a previous paper [9] for different lay-ups.

2 Materials, geometry and testing

Tubes with lay-up $[0_F/90_{U,3}/0_F]$ (FUF) are tested under different values of the biaxiality ratio $\lambda_{12} = \tau_{12}/\sigma_2$ in the 90° plies, in order to analyze its influence on the damage onset and propagation in these layers. Comparisons are made with previous results, [9], on tubes with lay-up $[90_{U,4}]$ (UD) and $[0_F/90_{U,3}]$ (FU). Subscripts *U* and *F* stand for *UD* and *Fabric* respectively.
All kinds of tubes are produced by mandrel wrapping and cured in autoclave (6 bars, 140°C, 1 hour). The internal and external diameters for the FUF specimens are 19 and 22 mm and the total and calibrated lengths are 150 and 70 mm respectively. The following materials are used:
- UE 400 REM by SEAL, G/E UD tape, thickness = 0.38mm, for the 90° UD plies;
- EE106-ET443 by SEAL, G/E fabric, thickness = 0.13mm, for the 0° fabric plies.

Fatigue tests are conducted with an axial-torsional MTS 809 testing system (load-controlled cycles, load ratio R = 0, frequency 10 Hz). Damage onset and evolution are monitored during the tests by an infrared camera FLIR SC7600 MW and by eye observations. When an UD lamina is subjected to a cyclic loading condition leading to a non-fiber-dominated response, it fails suddenly and without a progressive damage evolution. Conversely, if the same lamina is constrained between other layers with higher strength (i.e. 0° layers or fabric layers as in the present case), it undergoes multiple cracking and stable crack propagation. This allows us to

analyze with more accuracy the damage modes and their dependence on the biaxiality ratio in the specimens of the FUF and FU type, with respect to the UD ones. In addition, the damage nucleation in the 90° layers in the FUF tubes is insensitive to the surface finishing and surface defects, as instead may happen for FU and UD specimens.

3 Experimental results

3.1 S-N curves

In Fig.1 the S-N curves for UD tubes are plotted. Experimental data are taken from [9] and they correspond to the final failure of the unidirectional tubes. In fact, as stated above, no damage propagation or stiffness decrease is seen in this kind of specimens, and the first crack initiation immediately leads to an unstable propagation and complete failure. A strong detrimental effect due to the increasing shear stress component can be clearly observed, and it seems to be more pronounced for $\lambda_{12} > 1$.

A very similar trend is observed for the FUF specimens, whose results are presented in Fig. 2 in terms of the first visible crack nucleation, which is in this case followed by a stable propagation (see paragraph 3.2). It has been observed that the life spent for the first crack initiation varies from 20 to 70% of the total fatigue life for the FUF tubes. Complete failure in this case is controlled by the fatigue resistance of the fabric layers.

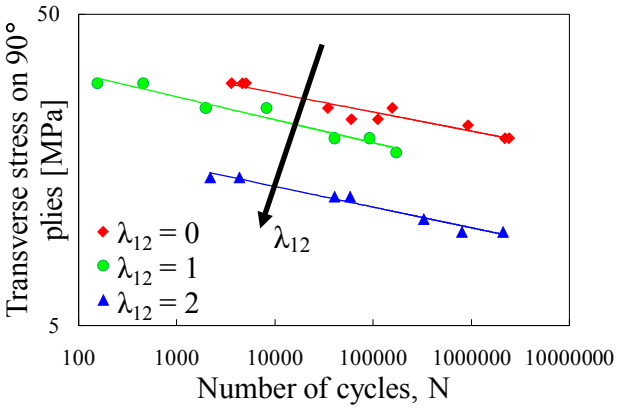

Fig.1 S-N curves for UD tubes

In Fig. 3 a comparison between the two types of tubes is shown. It is important to notice that the curves for the UD tubes slightly underestimate the fatigue resistance of the 90° layers in the FUF specimens in terms of first crack nucleation. This is due to the constraining effect of the stiffer fabric layers (increasing the in-situ strength of the 90° plies) and the entity of this effect depends on both the number of 90° plies and the stiffness of the constraining fabric layers [10].

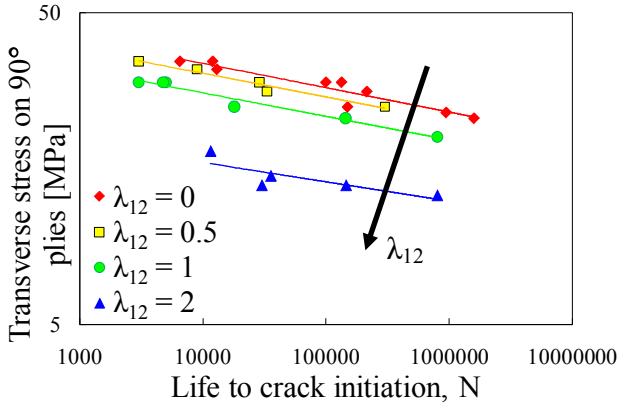

Fig.2 First crack nucleation data for FUF tubes

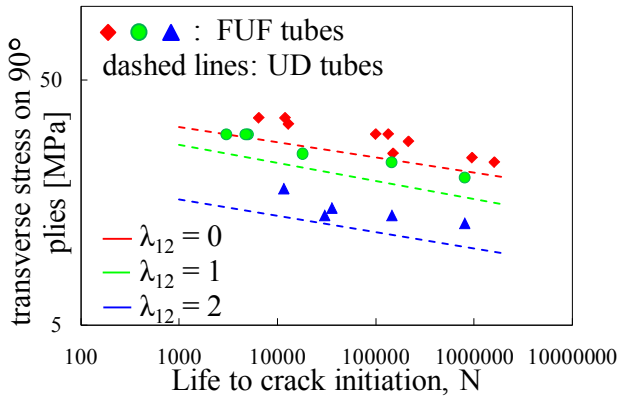

Fig. 3 Comparison between S-N curves for UD tubes (complete failure) and FUF tubes (first crack initiation)

3.2 Crack propagation

With the aim of understanding the influence of the shear stress on damage evolution, crack propagation is analyzed on FUF tubes in two phases. In the first phase the biaxiality ratio is varied with a fixed value of σ_2 on the 90° plies, while in the second one, different values of the transverse stress are applied

for the considered biaxiality ratios. Concerning the first phase, a maximum cyclic transverse stress of 30 MPa is kept constant, varying the biaxiality ratio (and thus the applied shear stress) from 0 to 1,5. Propagation curves are obtained by measuring the nucleated cracks during fatigue life. In Fig. 4 the angle of propagation, calculated as (2α - $2\alpha_i$), where $2\alpha_i$ is the initial crack angle at the moment of its identification, is plotted against the number of cycles of propagation. As a first approximation, the average Crack Growth Rate (CGR) is calculated as the slope of the straight line fitting each propagation curve for the various λ_{12}. The slope of the curves, i.e. the CGR, increases with increasing the shear stress contribution. Qualitatively similar propagation curves have been reported in [9], where the FU specimens were subjected to a maximum cyclic transverse stress of 23.7 MPa, with λ_{12} varying from 0 to 2.5. The average CGRs for FU tubes are higher than in the present case, though they are subjected to a lower stress state. This is explained if the results are analyzed in terms of Strain Energy Release Rate, as shown later on. Crack propagation occurs in mixed mode I + II, which are associated respectively to tensile and torsional loading.

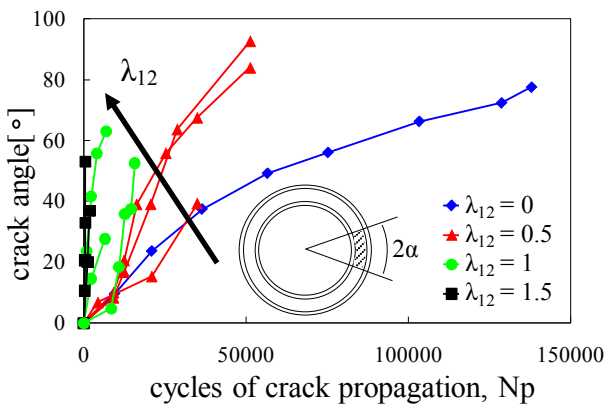

Fig.4 Crack propagation curves (maximum cyclic transverse stress = 30 MPa)

The mode I and II components of G are calculated via FE analyses of a cracked tube subjected to pure tension and torsion loadings, by means of the software ANSYS 11, using 20 nodes solid elements SOLID186. Circumferentially, 360 divisions are employed, while the 0° and 90° plies are divided in one and three elements respectively in the radial direction. Only one half of the tube is modelled with different crack angles (Fig. 5), and the compliance method is used for SERR calculation, with equations (1a and b):

$$G_I = \frac{F^2}{2}\frac{dC_I}{dA}, \qquad (1a)$$

$$G_{II} = \frac{T^2}{2}\frac{dC_{II}}{dA} \qquad (1b)$$

where A is the cracked area and F and T are the tensile and the torsion loads respectively.
Axial and tangential constrains are applied on the non-cracked portion of the front surface of Fig.5, so that the crack is simulated as a non constrained area on 90° plies only. Tension and torsion loading conditions are simulated by applying a uniform axial displacement on the back surface and a uniform tangential displacement on the external circumference of the back surface respectively.

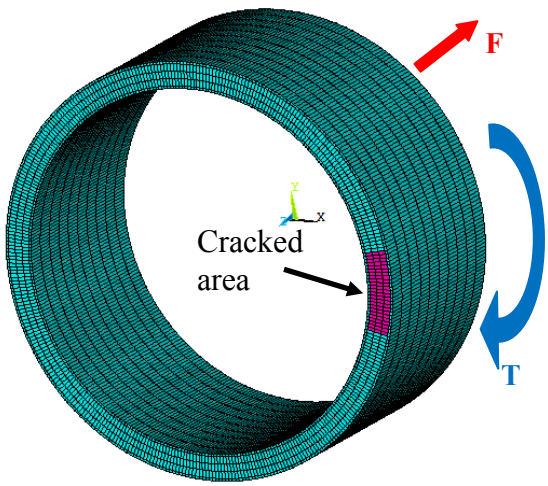

Fig. 5 FE model of a cracked tube

When a cracked ply is constrained between other layers, in a flat coupon under mode I, the SERR value reaches a plateau after a crack length about twice the layer thickness [11]. According to Eq. (1a and b), this means that the compliance's derivative with respect to the crack area becomes pretty constant. A similar trend is found even in the tubes investigated here, both for FU and FUF types. In Fig. 6 a) and b) the derivative of the compliance is plotted as a function of the crack angle for the FUF

tubes. In this case the steady-state propagation condition is reached for angles of 5-10° in mode I and 15-20° in mode II.

Since crack propagation occurs mainly in the plateau region, a single value of G_I and G_{II} has to be associated to each of the propagation curves in Fig. 4, both for FU and FUF tubes. A Mode Mixity (MM) parameter is defined as the ratio between G_{II} and the total value of SERR $G_{tot} = G_I + G_{II}$. By keeping G_I constant and increasing the Mode Mixity, the average CGR increases, in a similar way for the two kinds of samples (Fig.7), showing a considerable effect of the shear stress even on crack propagation, mainly for Mode Mixity values higher than 0.6 (i.e. $\lambda_{12} > 1$). FU tubes are subjected to a higher SERR even though the stress level is lower, and this is due to reduced constraining effect of the single internal fabric layer with respect to the case of FUF tubes where the 90° plies are constrained from both the internal and external fabric layers.

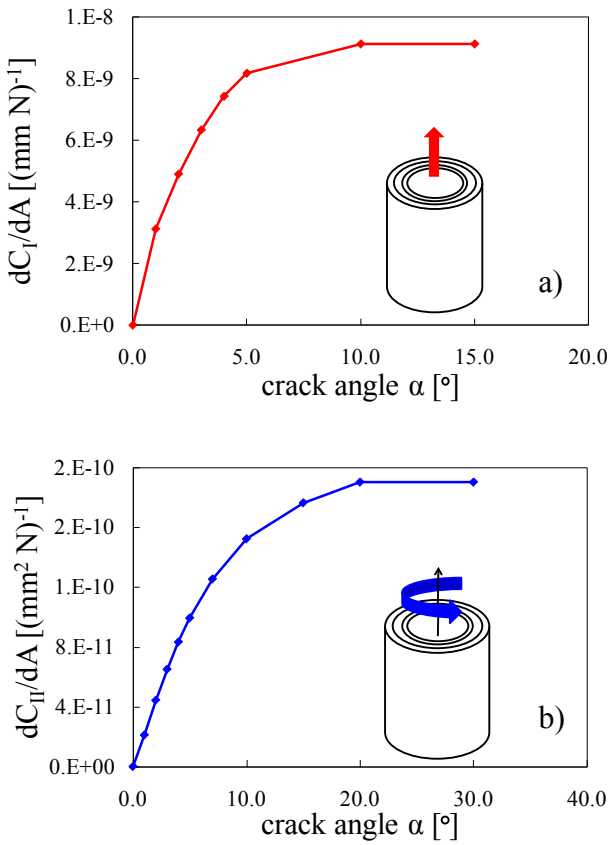

Fig. 6 Compliance derivative with respect to the crack area for a) mode I and b) mode II loadings

In this first phase, the propagation analysis has been carried by keeping a constant value of the transverse stress on 90° plies, and therefore of the mode I SERR, and an increase of the CGR has been observed increasing the mode II contribution. This result confirms clearly that G_I only is not a suitable parameter to describe crack propagation in a transverse UD ply under multiaxial loadings.

As said above, the second step of the analysis is conducted by changing the σ_2 level for every biaxiality ratio considered.

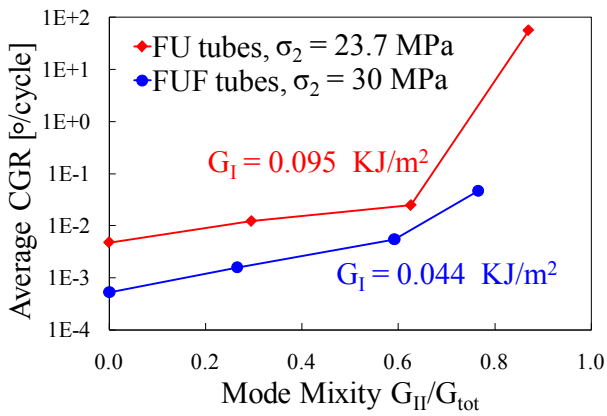

Fig. 7 Average CGR vs mode mixity for a fixed G_I, for FU and FUF samples

Some preliminary results are shown in Fig. 8 for λ_{12} = 0, 0.5, 1 (MM = 0, 0.26, 0.59), where the CGR is plotted as a function of the total SERR. Every point corresponds to one propagating crack. Most of specimens undergo multiple cracking, and therefore more than one point can be obtained from the same specimen, if the considered cracks are far enough from each other and thus non interacting.

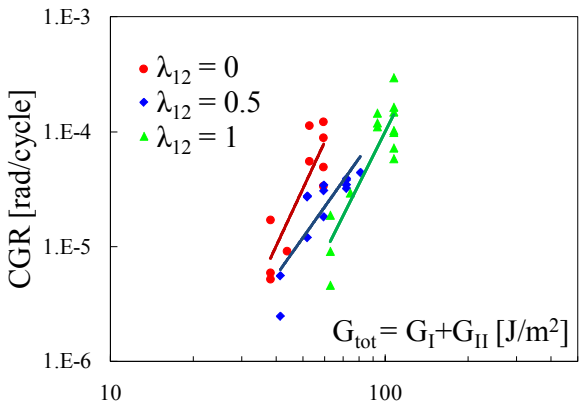

Fig.8 CGR vs total SERR

In spite of the scatter of data, it can be seen that different curves correspond to different values of λ_{12}, and therefore of the MM, and increasing the mode II contribution they shift from left to right. This reminds a well known trend for the interlaminar toughness of composite materials or bonded joints [12, 13, 14] subjected to mixed mode fatigue loading. In fact, the Paris curves for interlaminar fatigue crack propagation in terms of G_{tot} are usually more and more shifted to higher values of G as the MM is closer to 1. This means that, to obtain the same value of the CGR, a higher value of the total SERR is required as the pure mode II condition is approached. The reason for this is usually a change in the damage/propagation mode in the case of high shear stress contribution. In fact a crack subjected to a mixed mode loading condition tends to grow in a direction which is different to that of the pre-existing crack, but in the case of an interfacial crack in a bonded joint, for example, it has to remain straight and parallel to the interface. This causes the adhesive failure in the vicinity of the crack tip by means of microcracks which are perpendicular to the first principal stress direction [13, 15]. It is reasonable that a similar phenomenon occurs even for matrix cracks in the 90° layers, being them forced to remain parallel to the fibers (a higher energy would be required to bow through the fibers and change the growing direction). This idea seems to be supported by SEM observation of the fracture surfaces.

4 Fracture surface analysis

SEM analysis indicates that for low values of λ_{12} (0 and 0.5) the fracture surfaces are rather smooth. For λ_{12} = 1 shear cusps, which are typical of shear failure, start to appear, and they are widely present for λ_{12} = 2. All the samples show some clean fiber surfaces, suggesting that fiber-matrix debonding may play a role in the fracture process, however not being necessarily the leading damage mode. Even at a microscopic scale the damage modes are dependent on the multiaxiality condition, and a clear mechanism change is observed for λ_{12} greater than unity.

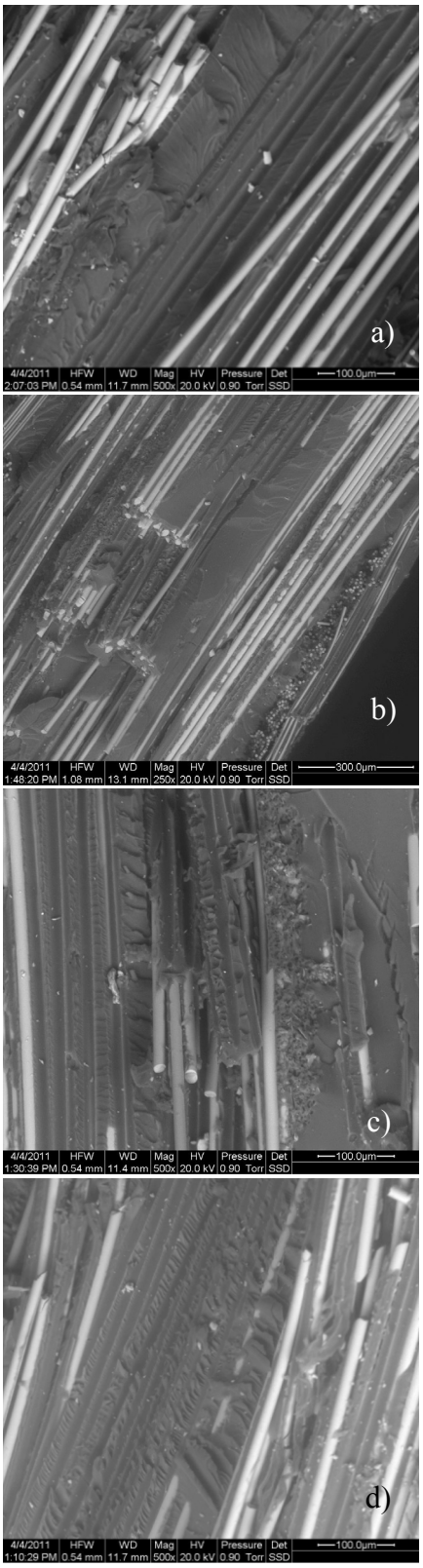

Fig.9 Fracture surfaces for a) λ_{12} = 0, b) λ_{12} = 0.5, c) λ_{12} = 1 and d) λ_{12} = 2

Conclusions

The behavior of G/E tubes under tension/torsion loading has been investigated and the main conclusions are as follows:

- A strong detrimental effect of the shear stress is found for damage onset and evolution;
- Crack nucleation resistance for FUF tubes is slightly higher than that for UD ones, this is attributed to the constraining effect of the internal and external fabric layers.
- Average CGR increases with increasing shear stress contribution for FU and FUF samples;
- Preliminary results seem to suggest that, plotting the CGR vs the total SERR, different curves are obtained, and they shift to higher SERR values as the mode mixity (i.e. the biaxiality ratio) increases;
- The external fabric layer on FUF specimens plays an important role in decreasing the SERR and therefore the CGR;
- Fracture surfaces and damage modes are seen to be strongly dependent on the biaxiality ratio.

References

[1] M. Quaresimin, L Susmel, R. Talreja, "Fatigue behaviour and life assessment of composite laminates under multiaxial loadings", *International Journal of Fatigue*, Vol. 32, pp 2-16, 2010.

[2] S. Adden, P. Horst, "Damage propagation in non-crimp fabrics under bi-axial static and fatigue loading". *Composites Science and Technology*, Vol. 33, pp 626-633, 2006.

[3] J. Tong, "Three stages of fatigue crack growth in composite laminates", *Journal of Engineering Materials and Technology,* Vol. 123, pp 139-143, 2001

[4] E. W. Smith, K. J. Pascoe, "Biaxial fatigue of glass-fibre reinforced composite. Part 1: fatigue and fracture behaviour." *Biaxial and Multiaxial Fatigue*, Edited by M. Brown and K. J. Miller, EGF 3, Mechanical Engineering Publications, London 1989, pp367-396.

[5] K. Takemura, T. Fujii, "Fatigue strength and damage progression in a circular-hole-notched GFRP composite under combined tension/torsion loading", *Composites Science and Technology*, Vol. 52, pp 519-526, 1994.

[6] T. Fujii, F. Lin, "Fatigue behavior of a plain-woven glass fabric laminate under tension/torsion biaxial loading" *Journal of Composite Materials*, Vol. 29, pp 573-590, 1995.

[7] H. Kawakami, T. Fujii, Y. Morita, "Fatigue degradation and life prediction of glass fabric polymer composite under tension/torsion biaxial loadings." *Journal of Reinforced Plastics and Composites*, Vol. 15, pp 183-195, 1996.

[8] A. Inoue, T. Fujii, H. Kawakami, " Effect of loading path on mechanical response of a glass fabric composite at low cyclic fatigue under tension/torsion biaxial loading." *Journal of Reinforced Plastics and Composites,* Vol. 19, pp 111-123, 2000.

[9] Quaresimin M., Talreja R. "Fatigue behaviour of composite tubes under multiaxial loading" invited lecture at ICFC5 - 5th International Conference on Fatigue of Composites, October 15-18, 2010 Nanjing , China.

[10] J. Wang, B. Karihaloo," Optimum in situ strength design of laminates under combined thermal and mechanical loads", *Composite Structures*, Vol. 47, pp 635-641, 1999.

[11] S. Ho, Z. Suo, "Tunneling cracks in constrained layers", *Journal of Applied Mechanics*, Vol. 60, pp 890-894, 1993.

[12] M. Kenane, M. L. Benzeggagh, "Mixed mode delamination fracture toughness of unidirectional glass/epoxy composites under fatigue loading", *Composites Science and Technology*, Vol. 57, pp 597-605, 1997;

[13] P. A. Carraro, G. Meneghetti, M. Quaresimin, M. Ricotta, " Fatigue behaviour of composite bonded joints under mixed mode loading", *Proceeeding of 14 European Conference on Composite Materials (ECCM14)*, Budapest, 2010;

[14] M. Hojo, S. Matsuda, S. Ochiai, "Delamination fatigue crack growth in CFRP laminates under mode I and II loadings - effect of mesoscopic structures on fracture mechanism -", Proceedings of the International Conference on Fatigue on Composites, Paris, pp 15-26, 1997

[15] CH. Wang, "Mixed mode fracture of interface cracks", *Proceedings of the First Australasian Congress on Applied Mechanics: ACAM-96. Barton, ACT: Institution of Engineers,* Australia, pp 245-250, 1996.